

Lawrence Berkeley National Laboratory

LBL Publications

Title

Redistribution of Electron Equivalents between Magnetite and Aqueous Fe²⁺ Induced by a Model Quinone Compound AQDS

Permalink

<https://escholarship.org/uc/item/7c68j66s>

Journal

Environmental Science and Technology, 53(4)

ISSN

0013-936X

Authors

Peng, Huan

Pearce, Carolyn I

N'Diaye, Alpha T

et al.

Publication Date

2019-02-19

DOI

10.1021/acs.est.8b05098

Peer reviewed

1 **Redistribution of Electron Equivalents between Magnetite**
2 **and Aqueous Fe²⁺**

3 **Induced by a Model Quinone Compound AQDS**

4

5 Huan Peng^{1,2}, Carolyn I. Pearce³, Alpha T. N'Diaye⁴, Zhenli Zhu^{2,*}, Jinren
6 Ni¹, Kevin M.

7

8 Rosso³, Juan Liu^{1,*}

9

10 ¹The Key Laboratory of Water and Sediment Sciences, College of
11 Environmental Sciences and

12 Engineering, Peking University, Beijing 100871, China

13 ²State Key Laboratory of Biogeology and Environmental Geology, School of
14 Earth

15 Sciences, China University of Geosciences, Wuhan, Hubei 430074, China

16 ³Pacific Northwest National Laboratory, Richland, WA 99352, USA

17 ⁴Advanced Light Source, Lawrence Berkeley National Laboratory, Berkeley, CA
18 94720, USA

19

20

21

22

23

24 *Corresponding authors:

25 J. L.

26 Address: College of Environmental Sciences and Engineering, Peking University,
27 Beijing 100871,

28 China

29 Email: juan.liu@pku.edu.cn

30 Z. Z.

31 Address: State Key Laboratory of Biogeology and Environmental Geology,
32 School of Earth

33 Sciences, China University of Geosciences, Wuhan, Hubei 430074, China

34 Email: zlzhu@cug.edu.cn

35

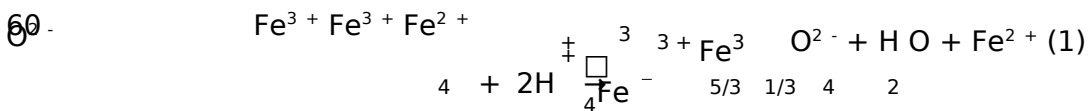
28 ABSTRACT:

29 The complex interactions between magnetite and aqueous Fe^{2+} ($\text{Fe}^{2+}_{(\text{aq})}$)
pertain to many
30 biogeochemical redox processes in anoxic subsurface environments. The effect
of natural organic
31 matter, abundant in these same environments, on $\text{Fe}^{2+}_{(\text{aq})}$ -magnetite
interactions is an additional
32 complex that remains poorly understood. We investigated the influence of a
model quinone
33 molecule anthraquinone-2,6-disulfonate (AQDS) on
 $\text{Fe}^{2+}_{(\text{aq})}$ -magnetite interactions by
34 systematically studying equilibrium $\text{Fe}^{2+}_{(\text{aq})}$ concentrations, rates and extents
of AQDS reduction,
35 and structural versus surface-localized Fe(II)/Fe(III) ratios in magnetite under
different controlled
36 experimental conditions. The equilibrium concentration of $\text{Fe}^{2+}_{(\text{aq})}$ in Fe^{2+} -
amended magnetite
37 suspensions with AQDS proportionally changes with solution pH or initial AQDS
concentration,
38 but independent of magnetite loadings through the solids concentrations that
were studied here.
39 The rates and extents of AQDS reduction by Fe^{2+} -amended magnetite
proportionally increased
40 with solution pH, magnetite loading, and initial $\text{Fe}^{2+}_{(\text{aq})}$ concentration, which
correlates with the
41 corresponding change of reduction potentials for the Fe^{2+} -magnetite system.
AQDS reduction by
42 surface-associated Fe(II) in the Fe^{2+} - magnetite suspensions induces solid-state
migration of
43 electron equivalents from particle interiors to the near-surface region and the
production of
44 non-magnetic Fe(II)-containing species, which inhibits $\text{Fe}^{2+}_{(\text{aq})}$ incorporation or
electron injection
45 into magnetite structure. This study demonstrates the significant influence of
quinones on
46 reductive activity of the Fe^{2+} -magnetite system.
47

48 **INTRODUCTION**

49 Magnetite (Fe₃O₄), one of the most common iron oxides, plays an
 important role in
 50 contaminant transformation, microbial extracellular respiration, and
 biogeochemical cycling of
 51 elements.¹⁻⁴ In addition, the growing use of magnetite for environmental and
 industrial
 52 applications may increase the release of synthetic magnetite into the
 environment.⁵⁻⁷ In anoxic
 53 subsurface environments magnetite can be formed from various
 biogeochemical processes, such
 54 as microbial or abiotic Fe(III) reduction and the weathering of Fe(II)-bearing
 minerals.^{8, 9} Its
 55 inverse spinel structure and mixed valent characteristics lead to a dynamic
 exchange of ferrous
 56 iron between the solid state and solution by topotactic oxidation/reduction
 processes.¹⁰ This
 57 exchange enables magnetite to encompass a range of stable stoichiometries
 that reflect a variable
 58 total oxidation state along a binary solid-solution with oxidized end-member
 maghemite, as

59 described by the equation below:¹¹



61 Thus, the complex equilibria between Fe²⁺_(aq) and magnetite can result in
 variable properties and
 62 redox reactivities of magnetite in natural environments.^{2, 3, 11-18} Although some
 efforts have been
 63 made to understand Fe²⁺_(aq)-magnetite interactions under environmentally
 relevant conditions,^{12-15,}
 64 ¹⁸most of them have focused on sorption behavior of Fe²⁺_(aq) onto magnetite
 of different
 65 stoichiometries¹⁴ or rates/extents of contaminant reduction by Fe²⁺_(aq)
 associated with magnetite
 66 nanoparticles.^{12, 13} Recent studies revealed that stable mineral recrystallization
 can happen when
 67 magnetite nanoparticles are exposed to Fe²⁺_(aq) in low-temperature (<100 °C)
 aqueous systems.^{15,}
 68 ¹⁹⁻²¹ However, few studies have addressed electron transfer processes between
 magnetite and

69 $\text{Fe}^{2+}_{(\text{aq})}$ under more complex environmental conditions. We recently examined the flow of electron

70 equivalents in the form of Fe(II) across the magnetite-solution interface and found that the

71 equilibrium between $\text{Fe}^{2+}_{(\text{aq})}$ and magnetite can be easily and reversibly influenced by fluctuations

72 in solution pH and $\text{Fe}^{2+}_{(\text{aq})}$ concentration.¹⁸ But the extent to which this applies to the less pristine

73 settings expected in more complex environmental systems has not yet been addressed.

74 For example, natural organic matter (NOM) may also affect $\text{Fe}^{2+}_{(\text{aq})}$ -magnetite interactions

75 via their redox-accessible functional groups, such as quinones,²²⁻²⁴ Moreover, many

76 microorganisms can use endogenous or exogenous quinone-like compounds as electron shuttles to

77 facilitate extracellular electron transfer with iron oxides at a distance.²⁵⁻²⁷ Both $\text{Fe}^{2+}_{(\text{aq})}$ and

78 magnetite can be formed from or participate in this process, so understanding the influence of

79 redox-active organics on $\text{Fe}^{2+}_{(\text{aq})}$ -magnetite interaction is important for mimicking the

80 biogeochemical complexity in more realistic anoxic subsurface environments. Previous studies

81 mainly focus on redox reaction between iron oxide and reduced quinones.^{22, 23, 28} To the best of

82 our knowledge, no studies have been reported about the influence of redox-active quinones on the

83 interaction between $\text{Fe}^{2+}_{(\text{aq})}$ and mixed-valent iron oxide. This furthermore applies to the

84 development of magnetite-based remediation strategies designed to exploit its high reduction

85 reactivity and simple magnetic separation.^{23, 29, 30} A magnetite coating often develops on the

86 surface of nanoscale zero-valent iron (nZVI), one of the most studied nanomaterials for the

87 remediation of subsurface contaminants.³¹⁻³³ The influence of ubiquitous redox-active organic

88 compounds on the effectiveness of these remediation strategies is not well known.

89 The objective of this study is to quantitatively assess the effects of redox-active organics on

90 the equilibrium distribution of electron equivalents, in the form of Fe(II), between $\text{Fe}^{2+}_{(\text{aq})}$ and

91 magnetite at pH 6-8. We selected anthraquinone-2,6-disulfonate (AQDS) as a model

92 quinone-containing, redox-active compound, which has been well studied and
 understood in the
 93 context as a biogeochemical electron shuttle. In the buffered aqueous
 solution at pH 6-8, the
 94 relevant redox equilibrium of AQDS (E_{AQDS}) is the pH-dependent two electron
 mass balance

95 between AQDS and AH_2DS given as:²³

$$96 \quad E_{AQDS} = E_{AQDS}^0 + \frac{RT}{2F} \ln \left([H^+]^2 + K_{a1}^{red} [H^+] + \frac{[AQDS_{red}]}{[AQDS]} \right) \quad (2)$$

97
 98 where $[AQDS_{red}]$ is total activity of the reduced AQDS species, including AH_2DS ,
 $AHDS^-$, and

99 $AQDS^{2-}$; K_{a1}^{red} and K_{a2}^{red} are the corresponding acid dissociation constants of the
 reduced forms of

100 AQDS. Based on the relationship between E_{AQDS} and equilibrium AQDS
 speciation, AQDS has
 101 been used as a non-sorbing chemical redox probe (CRP) to estimate reduction
 potentials of
 102 heterogeneous iron systems, consisting of $Fe^{2+}_{(aq)}$ and iron (oxyhydr)oxide.^{23, 24}
 However, it
 103 remains unclear whether or not this method can be applied to mixed-valent iron
 oxides such as
 104 magnetite, because the extent that CRPs are true spectator species that
 do not influence the
 105 distribution of electron equivalents across the magnetite-solution interface
 and thus its reduction
 106 potential is yet unknown.^{14, 34} Our results fill a knowledge gap in fundamental
 understanding of
 107 the effects of quinones on redox processes between $Fe^{2+}_{(aq)}$ and mixed-valent
 iron oxides, which
 108 has not been systematically studied.

109 In this study, equilibrium concentrations of $Fe^{2+}_{(aq)}$ were measured as a
 function of: (i)
 110 solution pH; (ii) initial $Fe^{2+}_{(aq)}$ concentrations ($[Fe^{2+}_{(aq)}]_{int.}$); (iii) magnetite
 loading; and (iv) initial
 111 AQDS concentration ($[AQDS]_{int.}$).³⁵ In addition, reduction kinetics and
 equilibrium speciation of
 112 AQDS with Fe^{2+} -amended magnetite under the corresponding experimental
 conditions were also

113 studied using UV-visible (UV-vis) absorption spectroscopy. Moreover, the changes of structural

114 Fe(II)/Fe(III) ratios in magnetite interiors and at particle surface after reaction
with $\text{Fe}^{2+}_{(\text{aq})}$ and

115 AQDS were quantified using micro X-ray diffraction (μXRD) and synchrotron-
based Fe *L*-edge

116 X-ray absorption (XA) and X-ray magnetic circular dichroism (XMCD)
spectroscopies,

117 respectively.^{2, 11, 16, 18} The systematic quantification of compositional changes
in both magnetite

118 particles and the aqueous solution revealed a significant influence of AQDS
on the equilibrium

119 distribution of electron equivalents in the form of Fe(II) under various
environmentally relevant

120 conditions, which may help us understand the reactivity of $\text{Fe}^{2+}_{(\text{aq})}$ -magnetite
systems in

121 subsurface environments.

122

123 MATERIALS AND METHODS

124 Magnetite synthesis and all wet chemical experiments were conducted
inside an anoxic

125 glovebox. All syringe filters, glassware, and plastic were deoxygenated for at
least 24 h inside the

126 glovebox prior to use. The details of the glovebox, degassed and deionized
water (DDW), and all

127 chemicals for magnetite synthesis and wet chemical experiments were
described in the Supporting

128 Information (SI Section 1).

129 **Magnetite synthesis and characterization.** Magnetite was synthesized
using the

130 co-precipitation method that was previously reported.^{11, 18} The resulting
particles were

131 magnetically separated from the aqueous phase and washed with DDW for
three times to remove

132 residual metal chlorides. After the washing processes, the particles were re-
suspended in DDW (~

133 300 mL) and stored in a sealed bottle covered with aluminum foil and
inside the glovebox.

134 Particle density of the stock suspension, in terms of equivalent Fe(II)
concentration, was measured

135 using an acid digestion method.^{2, 18} The crystal phase, size, morphology, and
specific surface area

136 of the synthetic particles were characterized by micro X-ray diffraction
(μ XRD), transmission
137 electron microscope (TEM), and Brunauer-Emmer-Teller (BET) method,
respectively. More
138 details about magnetite synthesis and characterization are provided in SI
Section 2.

139 **Quantification of equilibrium concentrations.** Batch experiments
were conducted to
140 measure final concentrations of $\text{Fe}^{2+}_{(\text{aq})}$ in the magnetite suspensions (69
- 695 mg L^{-1} , the
141 equivalent $\text{Fe}(\text{II})$ concentration of 300 - 3000 μM) after equilibration with 0 -
1000 μM $\text{Fe}^{2+}_{(\text{aq})}$
142 and 0 - 500 μM AQDS at pH 6 - 8 were measured. The buffer solution at pH 7
or 8 was 30 mM
143 HEPES (4-(2-hydroxyethyl)-1-piperazineethanesulfonic acid, 99.5%) solution,
and that at pH 6
144 was 30 mM MES (2-(N-Morpholino) ethanesulfonic acid, 99%) solution. The
buffers were
145 selected, because they have a low capability to complex with metal ions or
adsorb onto iron oxide
146 surface.^{36, 37} All experiments were conducted in sealed containers with
continuous shaking at 10
147 rpm using a rotating mixer in the glovebox. Batches with desired magnetite
loading and FeSO_4
148 concentration at a given pH were continuously shaken for 24 h in order to
allow the
149 $\text{Fe}^{2+}_{(\text{aq})}$ -magnetite system to reach equilibrium.¹⁴ Then, a certain volume of
AQDS stock solution
150 was spiked into the suspension that was shaken for another 24 h, until a new
equilibrium state was
151 established. Finally, the suspensions were filtered using 0.2 μm Nylon syringe
filters (Whatman),
152 and the first ~ 1 mL filtrate was discarded as a rinse. $\text{Fe}^{2+}_{(\text{aq})}$ concentration and
AQDS speciation in
153 the filtrates were measured, respectively, using the ferrozine assay³⁵ and the
UV-VIS absorption
154 spectra that were recorded using a Shimadzu UV-2501 PC spectrophotometer
inside the glovebox.
155 Within the pH range (pH 6-8) of this study, the interference of Fe^{3+} on the
measurements of
156 $\text{Fe}^{2+}_{(\text{aq})}$ by the ferrozine assay is negligible. The initial volume in all
experiments was 10 mL, and

157 all experiments were performed at least in triplicate.

158 **AQDS reduction kinetics.** Reduction kinetics of 100 μM AQDS by
magnetite (300 - 3000
159 μM [Fe(II)] equivalents) amended with 0 - 1000 μM $\text{Fe}^{2+}_{(\text{aq})}$ at pH 7 - 8
were measured by
160 monitoring the change of AQDS absorbance at 328 nm as a function of time.<sup>22-
24, 38</sup> No
161 experiments were conducted at pH 6, because no measurable AQDS was
reduced by 300-
3000
162 μM magnetite amended with 0-1000 μM $\text{Fe}^{2+}_{(\text{aq})}$ at this pH. At pH 7, reduction
experiments were
163 initiated by spiking a given volume of AQDS stock solution to a suspension of
magnetite
164 equilibrated with a certain concentration of $\text{Fe}^{2+}_{(\text{aq})}$. Sample aliquots (2 mL)
were taken using 10
165 mL syringes at desired time intervals and immediately filtered using 0.2 μm
syringe filters. The
166 absorbance spectra of the filtrates were recorded using the Shimadzu UV-
2501 PC
167 spectrophotometer inside the glovebox. At pH 8, AQDS reduction by Fe^{2+} -
amended magnetite
168 finished within several minutes, so the absorbance at 328 nm,^{22, 23, 38} instead of
the whole
169 spectrum, was recorded over time using the UV-VIS spectrophotometer at
an interval of 0.2
170 seconds. The reduction experiments were initiated by spiking a certain
volume of AQDS into
171 Fe^{2+} -amended magnetite suspensions in a 3.5 mL screw-cap quartz cuvette
that was capped and
172 placed in a Peltier cell holder with a stirring system. Dilute particle
suspensions were used in all
173 experiments, so there was no detectable interference from light scattering by
magnetite particles.
174 The concentration of reduced AQDS (C_t) at time t (min) was calculated using
the difference in
175 absorbance at 328 nm (oxidized form of AQDS).^{22, 23, 38} The first-order rate
constant (κ , min^{-1})
176 during the initial reaction stage of AQDS reduction by $\text{Fe}^{2+}_{(\text{aq})}$ -amended
magnetite under different
177 experimental conditions was calculated using the following equation:

178
$$\ln((C_0 - C_t)/C_0) = \kappa \cdot t \quad (3)$$

179 Where C_0 is the initial concentration of oxidized AQDS. All experiments were carried out at least

180 in triplicate. Because the reduction potentials of pure or Fe²⁺-amended
magnetite are lower than
181 that of reduced AQDS at the conditions present in our experiments (as
discussed below), no
182 experiments with pre-reduced AQDS in the Fe²⁺-magnetite systems were
conducted.

183 **Measurements of Fe(II)/Fe(III) ratios in magnetite.** The crystalline
phase and cell
184 parameters of magnetite in suspensions before and after reaction with Fe²⁺
(_{aq}) and AQDS were
185 measured by μ XRD. According to the linear correlation between the cubic unit
cell parameter (a)
186 and the structural Fe(II)/Fe(III) ratio (x_{stru}) in magnetite,¹¹ the change in x_{stru} of
magnetite after
187 reaction with Fe²⁺(_{aq}) and AQDS was determined from the refined unit-cell
parameters. Details
188 about μ XRD measurements and cell parameter refinement were described in SI
Section 2 and our
189 previous studies.^{2, 11, 18}

190 X-ray Magnetic Circular Dichroism (XMCD) was conducted to characterize
the oxidation
191 state and local structure of magnetically ordered iron cations at magnetite
surface (in the
192 outermost few Ångstroms of particle surface). The synchrotron XMCD spectra
of magnetite were
193 collected at room temperature on beamline 6.3.1 at the Advanced Light
Source (ALS), Berkeley,
194 CA, using the eight-pole resistive magnet end-station. A nonlinear least-squares
analysis of
195 XMCD spectra was conducted to quantify surface-localized Fe(II)/Fe(III) ratios
(x_{surf}) of
196 magnetite as described in previous studies.^{2, 11, 18}

197

198 **RESULTS AND DISCUSSION**

199 TEM images (Figure S1) showed that the synthetic nanoparticles were
nearly spherical with a
200 diameter of 12 ± 2 nm. The BET specific surface area of the nanoparticles
was 55.7 m²/g. The
201 XRD pattern (Figure S2) indicated that magnetite was the only phase
present in the synthetic

202 nanoparticles.

203 **Effects of AQDS on the equilibrium between magnetite and $\text{Fe}^{2+}_{(\text{aq})}$.** Our previous study

204 shows that, in the absence of AQDS, $\text{Fe}^{2+}_{(\text{aq})}$ release from magnetite is more favorable at pH 6 - 7

205 due to proton-promoted dissolution of magnetite, while $\text{Fe}^{2+}_{(\text{aq})}$ uptake by magnetite is more

206 feasible at pH 8.¹⁸ In addition to solution pH, addition of $\text{Fe}^{2+}_{(\text{aq})}$ can also evidently affect the

207 reactions at the magnetite-solution interface, resulting in the inhibited dissolution at pH 6 - 7 but

208 the increased $\text{Fe}^{2+}_{(\text{aq})}$ uptake at more basic conditions. Increasing magnetite loading enhanced the

209 extent of $\text{Fe}^{2+}_{(\text{aq})}$ -magnetite interaction by providing more available surface sites.¹⁸

210 Correspondingly, the structural and surface-localized Fe(II)/Fe(III) ratios of magnetite changed as

211 a result of the dynamic $\text{Fe}^{2+}_{(\text{aq})}$ -magnetite interaction. These findings revealed the reversible flow

212 of Fe(II) across the magnetite-solution interface under different conditions.¹⁸

213 To study the effect of AQDS on the equilibrium distribution of electron equivalents in the

214 $\text{Fe}^{2+}_{(\text{aq})}$ -magnetite system, equilibrium concentrations of $\text{Fe}^{2+}_{(\text{aq})}$ ($[\text{Fe}^{2+}_{(\text{aq})}]_{\text{eq}}$) in the magnetite

215 suspensions (69 - 695 mg L⁻¹) amended with 0 - 1000 μM $\text{Fe}^{2+}_{(\text{aq})}$ before and after the addition of

216 100 μM AQDS at pH 6 - 8 were measured (Figure S3). Figure 1 shows the difference between

217 equilibrium ($[\text{Fe}^{2+}_{(\text{aq})}]_{\text{eq}}$) and initial $\text{Fe}^{2+}_{(\text{aq})}$ ($[\text{Fe}^{2+}_{(\text{aq})}]_{\text{int.}}$) concentrations (i.e., $\Delta[\text{Fe}^{2+}_{(\text{aq})}] =$

218 $[\text{Fe}^{2+}_{(\text{aq})}]_{\text{eq}} - [\text{Fe}^{2+}_{(\text{aq})}]_{\text{int.}}$) as a function of magnetite loading under various experimental conditions.

219 At pH 6, the addition of 100 μM AQDS barely changes $[\text{Fe}^{2+}_{(\text{aq})}]_{\text{eq}}$ or $\Delta[\text{Fe}^{2+}_{(\text{aq})}]$ under the

220 conditions of the present study. The dominant interfacial reaction at pH 6 is proton-promoted

221 dissolution of magnetite, which leads to the release of 80.7-575.3 μM Fe^{2+} from 300-3000 μM

222 magnetite (Figure 1). Correspondingly, the structural Fe(II)/Fe(III) ratio and reduction reactivity

223 of magnetite decrease after the release of Fe^{2+} . As mentioned above, no

detectable AQDS is

224 reduced by Fe²⁺-amended magnetite (300-3000 μM magnetite, 0-1000 μM Fe²⁺_(aq)) at pH 6. Thus,

225 AQDS is unlikely to be reduced by the partially dissolved magnetite, even with
the released Fe²⁺

226 at pH 6 under the conditions of this study. As a non-sorbing redox
molecule for iron oxide

227 minerals,²³ AQDS shows no significant impacts on the equilibrium of the non-
redox dissolution

228 reaction.

229 At pH 7 without added Fe²⁺_(aq), addition of 100 μM AQDS does not
significantly change the

230 amount of released Fe²⁺ ($\Delta[\text{Fe}^{2+}_{(\text{aq})}]$) (Figure 1A). Only a very small amount
(0.6-6.7 μM) of

231 AQDS was reduced at the end of the experiments at pH 7 (Figure S4). Proton-
promoted

232 dissolution of magnetite is still the dominant interfacial reaction in this case,
and the presence of

233 100 μM AQDS did not obviously affect the extent of magnetite dissolution at
pH 7. However,

234 addition of 100 μM AQDS significantly decreased the value of $[\text{Fe}^{2+}_{(\text{aq})}]_{\text{eq}}$ in Fe²⁺-
amended

235 magnetite (Figure S3). Because AQDS cannot be reduced by dissolved Fe²⁺ at
pH 7,²⁴ the

236 observed decrease in $[\text{Fe}^{2+}_{(\text{aq})}]_{\text{eq}}$ cannot simply be attributed to Fe²⁺_(aq)
oxidation by AQDS. The

237 production of reduced AQDS (Figure S4) and the corresponding change of the
structural

238 Fe(II)/Fe(III) ratio (x_{stru}) in magnetite (Figure 2) after the addition of AQDS
suggest that the

239 decrease of $[\text{Fe}^{2+}_{(\text{aq})}]_{\text{eq}}$ is probably related to the redistribution of electron
equivalents in the

240 Fe²⁺-magnetite system induced by AQDS, which will be discussed further
below. In particular,

241 $\Delta[\text{Fe}^{2+}_{(\text{aq})}]$ changes from positive to negative values (when $[\text{Fe}^{2+}_{(\text{aq})}]_{\text{int}} = 250$
- 750 μM) after

242 adding AQDS, suggesting that the flow direction of electron equivalents across
the

243 magnetite-solution interface changed from magnetite \square solution to solution \square
magnetite.

244 Although adding 1000 μM Fe²⁺_(aq) to 300-3000 μM magnetite suspensions
without AQDS at pH 7

can also result in the similar reversal of flow direction,¹⁸ the presence of 100 μM AQDS obviously

246 decreases the threshold concentration of $\text{Fe}^{2+}_{(\text{aq})}$ for the occurrence of this
phenomenon from 1000
247 μM to 250 μM or less. Thus, the presence of AQDS facilitates the flow of
electron equivalents
248 from the solution phase to the solid phase (i.e. magnetite).

249 At pH 8, no measurable Fe^{2+} was released from magnetite without added
 $\text{Fe}^{2+}_{(\text{aq})}$, no matter
250 whether AQDS was present. In the Fe^{2+} -magnetite system, AQDS is mainly
reduced by
251 surface-associated Fe^{2+} (Fe(II)-Mt), because the reduction rate by Fe(II)-Mt
($[\text{Fe}^{2+}_{(\text{aq})}]_{\text{int}} =$
252 500-1000 μM , 300 - 3000 μM magnetite is 3 - 5 orders of magnitude faster
than that of $\text{Fe}^{2+}_{(\text{aq})}$ or
253 $\text{Fe}(\text{II})_{\text{stru}}$ in magnetite under similar conditions (Table S1). Figure 1 shows that
addition of 100 μM
254 AQDS generally results in more negative values of $\Delta[\text{Fe}^{2+}_{(\text{aq})}]$ (i.e. a greater
decrease in $\text{Fe}^{2+}_{(\text{aq})}$
255 concentration) at pH 8 in $\text{Fe}^{2+}_{(\text{aq})}$ -amended magnetite. Moreover, much more
AQDS is reduced by
256 $\text{Fe}^{2+}_{(\text{aq})}$ -amended magnetite at pH 8 than at pH 7. The fast reduction of AQDS
by Fe(II)-Mt at pH
257 8 drive the flow of electron equivalents from solution to magnetite and
change the speciation of
258 AQDS, which will be discussed further with the XMCD and μXRD results below.

259 The presence of AQDS also changes the influence of magnetite loading on
 $\Delta[\text{Fe}^{2+}_{(\text{aq})}]$ at pH 7
260 and 8. In the absence of AQDS, the absolute value of $\Delta[\text{Fe}^{2+}_{(\text{aq})}]$ increases
linearly with the
261 increase of magnetite loading from 300 to 3000 μM at pH 6 - 8 (Figure 1),
probably due to more
262 surface sites available for $\text{Fe}^{2+}_{(\text{aq})}$ -magnetite interaction with the increase of
magnetite loading.¹⁸
263 However, in the presence of 100 μM AQDS, the absolute values of $\Delta[\text{Fe}^{2+}_{(\text{aq})}]$
only slightly
264 increases or fluctuates around a fixed value as magnetite loading increases,
when $[\text{Fe}^{2+}_{(\text{aq})}]_{\text{int.}}$ was
265 0 - 1000 μM at pH 7 or less than 750 μM at pH 8 (Figure 1). As shown in Figure
S4, the increase
266 of mineral loading results in more reduced AQDS, which probably offsets the
effect of increasing
267 mineral loading on $\Delta[\text{Fe}^{2+}_{(\text{aq})}]$.

268 At the same magnetite loading and initial $\text{Fe}^{2+}_{(\text{aq})}$ concentration, changing
initial AQDS
269 concentration ($[\text{AQDS}]_{\text{int.}}$) can also affect the equilibrium between magnetite
and $\text{Fe}^{2+}_{(\text{aq})}$. For
270 example, in the suspensions of 3000 μM magnetite with 1000 μM $\text{Fe}^{2+}_{(\text{aq})}$,
increasing $[\text{AQDS}]_{\text{int.}}$
271 from 100 to 500 μM significantly increases the absolute values of $\Delta[\text{Fe}^{2+}_{(\text{aq})}]$
(i.e. more Fe^{2+} ions
272 transfer from solution to solid) and the equilibrium concentrations of reduced
AQDS
273 ($[\text{AQDS}_{\text{red}}]_{\text{eq}}$) (Figure 3). Moreover, the change of $\Delta[\text{Fe}^{2+}_{(\text{aq})}]$ and $[\text{AQDS}_{\text{red}}]_{\text{eq}}$ with
the increase of
274 $[\text{AQDS}]_{\text{int.}}$ is more significant in the suspensions amended with $\text{Fe}^{2+}_{(\text{aq})}$ at the
elevated pH (Figure
275 3). These results show that the presence of AQDS generally decreases
equilibrium concentrations
276 of $\text{Fe}^{2+}_{(\text{aq})}$ ($[\text{Fe}^{2+}_{(\text{aq})}]_{\text{eq}}$) in the Fe^{2+} -magnetite system at pH 7-8. The extent of
this impact depends
277 on solution pH and initial AQDS concentration. However, the decrease of $[\text{Fe}^{2+}_{(\text{aq})}]_{\text{eq}}$
after addition
278 of AQDS can be related to electron injection from $\text{Fe}^{2+}_{(\text{aq})}$ to magnetite, or
electron transfer from
279 $\text{Fe}^{2+}_{(\text{aq})}$ to AQDS, or the change of $\text{Fe}^{2+}_{(\text{aq})}$ to surface-associated Fe^{2+} . The
rate and extend of
280 AQDS reduction and the change of Fe(II)/Fe(III) ratios in magnetite are needed
to illustrate the
281 flow of electrons in the Fe^{2+} -magnetite system with AQDS.

282 **AQDS reduction by Fe^{2+} -amended magnetite.** Kinetic profiles of AQDS
reduction by
283 Fe^{2+} -amended magnetite (300-3000 μM magnetite, 0-1000 μM added $\text{Fe}^{2+}_{(\text{aq})}$)
at pH 7 and 8 are
284 shown in Figure S5 and S6, respectively. In 3000 μM magnetite suspension
without added $\text{Fe}^{2+}_{(\text{aq})}$,
285 the initial rate of AQDS reduction at pH 8 is one order of magnitude greater
than that at pH 7
286 (Table S1). Reduction potentials of both $\text{AQDS}_{\text{ox}}/\text{AQDS}_{\text{red}}$ and magnetite/ Fe^{2+}
couples decrease
287 with increasing pH (Figure S7), but the magnetite/ Fe^{2+} couple has a steeper
negative slope (-236
288 mV/pH)³⁰ than that of $\text{AQDS}_{\text{ox}}/\text{AQDS}_{\text{red}}$ (-59 mV/pH),^{23, 28, 39} resulting in the
enhanced reduction

rates of AQDS at high pH. Our previous study shows that the bulk structural Fe(II)/Fe(III) (x_{stru})

290 in magnetite in the absence of AQDS is higher at pH 8 than that at pH 7, when
other experimental
291 conditions are same.¹⁸ Because reduction potential of magnetite is inversely
proportional to x_{stru} in
292 magnetite,²⁹ magnetite exhibits a higher reactivity for AQDS reduction at pH 8
than at pH 7.

293 Recent studies of contaminant reduction by Fe^{2+} in the presence of
Fe(III)-(oxyhydr)oxide
294 reported a linear relationship between the logarithms of the surface-area-
normalized reduction rate
295 constants and reduction potentials for oxide-bound Fe^{2+} species, when
electron transfer at the
296 solid/solution interface occurs during or before the rate-limiting step of the
reactions.^{24, 40} This
297 linear free energy relationship (LFER) is also observed in our study. In
Figure S8, the
298 surface-normalized rate constants ($\log k_{SA}$, data shown in Table S2) for AQDS
reduction were
299 plotted versus the reduction potential (E_H) of magnetite suspension (300 to
3000 μM magnetite)
300 equilibrated with 0 to 1000 μM added $Fe^{2+}_{(aq)}$ at pH 7 and 8. The E_H value of
magnetite suspension
301 was calculated from the measured $[Fe^{2+}_{(aq)}]_{eq}$ using the Nernst equation for
the following
302 half-reaction (for more details about E_H calculation, refer to SI section 3):^{18, 40, 41}

$$303 \quad 0.5Fe_3O_4 + 4H^+ + e^- \rightarrow 1.5Fe^{2+} + 2H_2O \quad (4)$$

304 A good linear correlation is observed between $\log k_{SA}$ and E_H for Fe^{2+} -amended
magnetite at pH 7
305 and 8 (Figure S8), suggesting that the rates of AQDS reduction by Fe^{2+} -
amended magnetite are
306 limited by electron transfer across the magnetite-solution interface. On the
other hand, the rates of
307 AQDS reduction significantly increase with the increase of solution pH,
magnetite loading, or
308 $[Fe^{2+}_{(aq)}]_{int}$. (Table S1). For example, as magnetite loading increases from 300 to
3000 μM , the
309 reduction rate of AQDS by magnetite amended with 1000 μM $Fe^{2+}_{(aq)}$
increases two orders of
310 magnitude. The observed faster reduction rates of AQDS reflect the decrease
of E_H for
311 Fe^{2+} -amended magnetite with the change of these experimental conditions.

312 The absorbance spectra of AQDS after reaction with Fe²⁺-amended
magnetite at pH 7 - 8

313 (Figure S9) confirmed that AQDS reduction under these conditions is a two-
electron transfer

314 reaction. As shown in Equation 2, AQDS reduction is a pH-dependent reaction.
When pH < pK^{red}_a

315 (the acidity constant for the reaction from AQDSH₂ to AQDSH⁻), AQDS
reduction involves

316 two-electron transfer.⁴² Although the p^{red}_{a1} value varies (pH 7.2-8.7) in literature, the
value of 8.1

317 has been widely used for pK^{red}_a.^{22-24, 43} The observed spectra in Figure S9 are
consistent with the

318 previous studies.^{23, 38, 44} To study electron balance of the reactions, the change
of Δ[Fe²⁺_(aq)] (δ =

319 Δ[Fe²⁺<sub>(aq)]_{without AQDS} - Δ[Fe²⁺<sub>(aq)]_{with AQDS}) in Fe²⁺-amended magnetite before and
after reaction</sub></sub>

320 with AQDS ([AQDS]_{int.} = 100 μM) was compared to the amount of electrons
transferred to AQDS

321 (2*[AQDS]_{red,eq}) (Figure S10). At pH 7, the values of δ are generally greater
than the

322 corresponding values of 2*[AQDS]_{red,eq}, whereas at pH 8 the latter is greater in
the suspensions

323 amended with 0 - 500 μM Fe²⁺_(aq). In all of these experiments, the values of δ
and 2*[AQDS]_{red,eq}

324 are generally different, (Figure S10) suggesting that the change of Δ[Fe²⁺_(aq)]
after adding AQDS

325 cannot simply be attributed to AQDS reduction by Fe²⁺_(aq). Redistribution of
electron equivalents

326 between magnetite and aqueous phase may be induced by the addition of
AQDS, which will be

327 discussed together with the changes in the Fe(II)/Fe(III) ratios of magnetite.

328 **Changes of Fe(II)/Fe(III) ratios in magnetite.** The μXRD patterns of
all post-reaction

329 samples show that no secondary crystalline phases were produced under all
experimental

330 conditions, but the unit-cell parameter of magnetite changed after
reaction. The values of

331 structural Fe(II)/Fe(III) ratio in magnetite (x_{stru}) derived from the μXRD patterns
of magnetite (69

332 - 695 mg L⁻¹) after reaction with 0 - 1000 μM Fe²⁺_(aq) and 100 μM AQDS at
pH 7 and 8 are

333 compared in Figure 3 (data shown in Table S3). The results indicate that X_{stru} systematically

334 increases with solution pH, magnetite loading, and $[\text{Fe}^{2+}_{(\text{aq})}]_{\text{int.}}$. Due to the
negative linear

335 relationship between reduction potential and x_{stru} value for the magnetite-
maghemite (Fe_3O_4 -

336 $\text{Fe}_{8/3}\text{O}_4$) system,⁴⁵ the higher x_{stru} values at the increased solution pH, magnetite
loading, or

337 $[\text{Fe}^{2+}_{(\text{aq})}]_{\text{int.}}$ imply the lower reduction potential for magnetite as these
conditions change. It is

338 worth mentioning that the decrease of x_{stru} value upon addition of magnetite
into the buffer

339 solutions at pH 7 or 8 is due to the pH difference between the stock suspension
of magnetite (~ 8.5)

340 and the buffer solutions.^{11, 18} Spiking an aliquot of the stock suspension into
the buffer solution

341 can result in a sudden pH decrease, which can induce Fe^{2+} release or solid-
state migration of

342 electrons from the interior to the near-surface region. The changes of x_{stru}
values with solution pH,

343 magnetite loading, and $[\text{Fe}^{2+}_{(\text{aq})}]_{\text{int.}}$ in the suspensions without AQDS were
reported and discussed

344 in our previous study.¹⁸

345 Because the electrochemical determination of redox potential for Fe^{2+} -iron
oxide redox

346 couple in aqueous suspension is still quite challenging, due to the influences of
many factors, such

347 as particle aggregation, mass transport, lack of redox equilibria, and formation
of secondary

348 phases,^{24, 46} recent studies proposed a method for the estimation of reduction
potential for

349 Fe^{2+} -iron oxide redox couples using CRPs, like AQDS.^{23, 24, 47} According to this
method, reduction

350 potentials for Fe^{2+} -amended magnetite ($E_{\text{Fe(II)} - \text{Mt}}$) under different conditions
can be calculated

351 from $[\text{AQDS}_{\text{red}}]_{\text{eq}}$ and $[\text{AQDS}]_{\text{int.}}$, as shown in Figure S11 (for more details
about $E_{\text{Fe(II)} - \text{Mt}}$

352 calculation, see SI Section 4). The results indicate that the values of $E_{\text{Fe(II)} - \text{Mt}}$ became
more

353 negative with the increase of magnetite loading, $[\text{Fe}^{2+}_{(\text{aq})}]_{\text{int.}}$, or pH (Figure S11),
which is

354 consistent with the trend in x_{stru} values for magnetite (Figure 3). It is worth
mentioning that, at the

355 same experimental condition, the
calculated

$E_{\text{Fe(II)}} -$
 M_t

is systematically higher than
the

356 calculated value of E_H (Figure S12). Because E_H was calculated mainly based on
pH and

357 $[\text{Fe}^{2+}_{(\text{aq})}]_{\text{eq}}$, the difference between $E_{\text{Fe(II)} - \text{Mt}}$ and E_H can be attributed to the changes of
magnetite

358 and the reduction of AQDS in the system (Figure 2 and 3).

359 As shown in Figure 2 and 3, different $[\text{AQDS}]_{\text{int.}}$ values result in different
values of x_{stru} ,

360 $[\text{Fe}^{2+}_{(\text{aq})}]_{\text{eq}}$, and $[\text{AQDS}_{\text{red}}]_{\text{eq}}$ in the suspensions of $\text{Fe}^{2+}_{(\text{aq})}$ -amended magnetite,
so the

361 correspond ing $E_{\text{Fe(II)} - \text{Mt}}$ values for Fe^{2+} -amended magnetite can be different with
the increase of

362 $[\text{AQDS}]_{\text{int.}}$ (Figure S11). For example, as $[\text{AQDS}]_{\text{int.}}$ increases from 100 to 500
 μM in the 3000

363 μM magnetite suspension amended with 1000 μM $\text{Fe}^{2+}_{(\text{aq})}$ at pH 8, $[\text{AQDS}_{\text{red}}]_{\text{eq}}$
changes from 95.8

364 to 368.7 μM (Figure 3), and correspondingly $E_{\text{Fe(II)} - \text{Mt}}$ increases from -277.8 to -250.8
mV

365 (Figure S11). On the other hand, $\Delta[\text{Fe}^{2+}_{(\text{aq})}]$ changes from -682 to -988 μM
(Figure 3), indicating

366 that the change of $[\text{Fe}^{2+}_{(\text{aq})}]_{\text{eq}}$ is less than the change of $2 \cdot [\text{AQDS}_{\text{red}}]_{\text{eq}}$
(546 μM). Thus, the

367 decrease of x_{stru} in magnetite (Table S3) with the increase of $[\text{AQDS}]_{\text{int.}}$ may be
related to AQDS

368 reduction by structural Fe(II) in magnetite. The results suggest that increasing
the initial

369 concentration of AQDS can increase the flow of $\text{Fe}^{2+}_{(\text{aq})}$ from solution to solid,
promote oxidation

370 of structural Fe(II) (i.e. the decrease x_{stru}) in magnetite, and increase the
reduction potential of the

371 Fe^{2+} -magnetite system ($E_{\text{Fe(II)} - \text{Mt}}$). Thus, $E_{\text{Mt} - \text{Fe(II)}}$ calculated from equilibrium
AQDS

372 speciation represents the reduction potential for the Fe^{2+} -magnetite system
after equilibration with

373 AQDS, which can be different from the value of the system before AQDS
addition. Caution must

374 be taken when comparing $E_{\text{Mt} - \text{Fe(II)}}$ values calculated from equilibrium
speciation of CRPs with

375 different initial concentrations. In addition, reduction potentials of mixed-valent
iron oxides, such

376 as magnetite and green rust, depend on the structural Fe(II)/Fe(III) ratio

(x_{stru}).²⁹ Even in the

377 reactions with other common CRPs, like carbon tetrachloride, 4-chloronitrobenzene (4-CINB),

378 and 2-chloroacetophenone, x_{stru} in the mixed-valent iron oxides may also
change as the reactions

379 proceed. For example, the reduction of 4-CINB by green rust was found to be
increasingly slower

380 over time, and correspondingly the reduction potential of the suspension
gradually increased.⁴⁸

381 X-ray absorption spectra indicate the increasing Fe(III) contents in green rust
during reaction,

382 suggesting that x_{stru} in green rust decreased during the reaction with 4-CINB.
Different types of

383 CRPs may with mixed-valent iron oxides to different extents, and
correspondingly the measured

384 reduction potentials from equilibrium speciation of CRPs may be different.

385 In addition to structural Fe(II)/Fe(III) ratio (x_{stru}) of magnetite, the oxidation
state and local

386 structure of magnetically ordered iron cations at the magnetite surface
(x_{surf}), before and after

387 reaction with $Fe^{2+}_{(aq)}$ and AQDS, were also analyzed using Fe L_{2,3}-edge XMCD.
Addition of 100

388 μM AQDS to magnetite suspensions ([Fe(II)] equivalents = 3000 μM) without
added $Fe^{2+}_{(aq)}$

389 increases x_{surf} at both pH 7 and pH 8 (Figure 4 and Table 1). The
corresponding structural

390 Fe(II)/Fe(III) ratio decreases after adding AQDS (Table 1), suggesting that
AQDS induces the

391 solid-state migration of electrons from the interior to the near-surface region
in magnetite under

392 these conditions. However, in the magnetite suspensions amended with 1000
 μM $Fe^{2+}_{(aq)}$, addition

393 of 100 μM AQDS obviously decreased x_{surf} at pH 7 and 8. The different
changes of x_{surf} values

394 after addition of AQDS in magnetite and Fe^{2+} -amended magnetite
suspensions suggest different

395 flow directions of electron equivalents in the system under different
conditions, as discussed

396 below.

397 **Redistribution of electron equivalents induced by AQDS.** To study
the effect of AQDS on

398 mass and electron balance in $Fe^{2+}_{(aq)}$ -magnetite interactions under different
experimental

399 conditions, $\Delta[Fe^{2+}_{(aq)}]$ and $[AQDS_{red}]_{eq}$, as well as x_{stru} and x_{surf} in magnetite,

before and after

400 addition of 100 μM AQDS are compared in Table 1. Because of the limited beam
time for XMCD

401 measurements, only some representative samples were analyzed using
XMCD. The x_{stru} value

402 (0.498) of 3000 μM magnetite in the pH 7 buffer solution without added $\text{Fe}^{2+}_{(aq)}$
was smaller than

403 that (0.544) of magnetite in the stock suspension (pH = ~ 8.5), due to the
release of 250.5 μM

404 $\text{Fe}^{2+}_{(aq)}$ from magnetite after transferring magnetite from the stock solution to
the buffer solution.

405 The value of $\Delta[\text{Fe}^{2+}_{(aq)}]$ (250.5 μM) measured from chemical analysis is
consistent with the

406 decrease (251 μM) of structural Fe(II) in magnetite ($[\text{Fe(II)}_{stru}]$) that is calculated
from the μXRD

407 results (for details of $[\text{Fe(II)}_{stru}]$ calculation, see SI section S5). Thus, in the
suspension without

408 added $\text{Fe}^{2+}_{(aq)}$ at pH 7, the increase of $[\text{Fe}^{2+}_{(aq)}]$ is mainly attributed to Fe(II)
release from

409 magnetite structure as a result of proton-promoted dissolution.¹⁸

410 Addition of 100 μM AQDS to the suspension under the same condition (pH
= 7, 3000 μM

411 magnetite) decreases the value of $\Delta[\text{Fe}^{2+}_{(aq)}]$ from 250.5 to 206.7 μM , and the
corresponding value

412 of $[\text{AQDS}_{red}]_{eq}$ is 6.7 μM (Table 1). There are 220.1 μM electron equivalents
transferred from

413 magnetite to the solution ($\Delta[\text{Fe}^{2+}_{(aq)}] + 2*[\text{AQDS}_{red}]_{eq}$ in Table 1). The
calculated decrease of

414 $[\text{Fe(II)}_{stru}]$ in magnetite after reaction with AQDS is ~ 287 μM (for details of Δ
 $[\text{Fe(II)}_{stru}]$

415 calculation, see SI Section S5.2), which is greater than the amount of electron
equivalents

416 transferred from magnetite to the solution ($\Delta[\text{Fe}^{2+}_{(aq)}] + 2*[\text{AQDS}_{red}]_{eq}$). The
decrease of x_{stru} and

417 the increase of x_{surf} in magnetite after addition of AQDS (Table 1) suggest solid-
state migration of

418 electrons from the particle interior to the near surface region induced by
AQDS reduction on

419 magnetite surface. This similar outward migration of electron equivalents in
magnetite structure

420 was observed in the reduction of pertechnetate anions ($[\text{TcO}_4^-]$) and a bacterial
enzyme MtoA by

421 magnetite.¹⁶ The calculated $[\text{Fe(II)}_{\text{stru}}]$ in the near-surface region is 319.4 μM higher than the value

422 before reaction with AQDS (SI section S5.2). Thus, the difference between
the calculated Δ

423 $[\text{Fe(II)}]_{\text{stru}}$ from μXRD and the amount of $(\Delta[\text{Fe}^{2+}_{(\text{aq})}] + 2*[\text{AQDS}_{\text{red}}]_{\text{eq}})$ can be
attributed to the

424 solid-state migration of electrons from the particle interior to the near surface
region. Although the

425 amount (250.5 μM) of Fe^{2+} released from 3000 μM magnetite at pH 7 is
theoretically sufficient for

426 complete reduction of AQDS (100 μM), only a limited amount (6.7%) of AQDS is
reduced in the

427 system (Table 1). It is possible that accessibility to structural and surface-
associated Fe(II) , and the

428 coupled diffusion of the electrons to maintain charge balance in the solid,
control the extent of

429 AQDS reduction. Thus, in magnetite suspensions without added $\text{Fe}^{2+}_{(\text{aq})}$ at pH 7,
the slight

430 reduction of AQDS by Fe(II) in magnetite structure inhibits magnetite
dissolution but induces

431 solid-state migration of electrons from the interior to the near-surface region of
magnetite.

432 The amendment of 1000 μM $\text{Fe}^{2+}_{(\text{aq})}$ to magnetite suspensions (3000 μM)
at pH 7 results in

433 the decrease of $\Delta[\text{Fe}^{2+}_{(\text{aq})}]$ (Table 1), due to inhibition of magnetite dissolution
by added $\text{Fe}^{2+}_{(\text{aq})}$.¹⁸

434 Addition of 100 μM AQDS changes $\Delta[\text{Fe}^{2+}_{(\text{aq})}]$ from positive to negative values,
and

435 correspondingly 98% AQDS is reduced by the Fe^{2+} -magnetite system. The
decrease of $[\text{Fe}^{2+}_{(\text{aq})}]_{\text{eq}}$

436 is much more than the value of $2*[\text{AQDS}_{\text{red}}]_{\text{eq}}$, so not all electrons are
transferred from $\text{Fe}^{2+}_{(\text{aq})}$ to

437 AQDS. Both x_{stru} and x_{surf} in magnetite decreased after addition of AQDS to the
 Fe^{2+} -magnetite

438 system (Table 1). The observed decrease of x_{stru} is probably attributed to solid-
state migration of

439 electrons from the interior to the near-surface region of magnetite due to
AQDS reduction by

440 surface-associated Fe^{2+} , which is similar to the phenomenon in magnetite
suspensions without

441 added $\text{Fe}^{2+}_{(\text{aq})}$. However, different from the case without added $\text{Fe}^{2+}_{(\text{aq})}$, x_{surf} of
magnetite amended

442 with 1000 μM $\text{Fe}^{2+}_{(\text{aq})}$ obviously decreases after AQDS addition, which might
be related to a

443 change of Fe(II) speciation on magnetite surface. XMCD is only sensitive to magnetically ordered

444 Fe(II) in the near-surface region of magnetite, but the XAS signal corresponds
to both magnetic
445 and non-magnetic Fe in the system. The intensity of Fe(II) peak in the XAS
signal did not
446 obviously decrease after addition of AQDS (Figure S13), suggesting the
formation of
447 non-magnetic Fe(II)(OH)₂-like species on magnetite surface in this case. This is
different from the
448 results of the Fe²⁺-magnetite system without AQDS, in which no stable Fe(II)
surface complexes
449 or secondary Fe²⁺ precipitates are formed.¹⁴ Further studies are needed to
investigate the effect of
450 AQDS on the complexation of Fe²⁺ on magnetite surface. There are no peaks of
secondary phases
451 in the μ XRD patterns of all post-reaction samples, indicating that the non-
magnetic
452 Fe(II)(OH)₂-like species is probably amorphous or at a quantity below the
detection limit of
453 μ XRD. The formation of Fe(II)(OH)₂-like species also makes it difficult to get a
closed
454 mass/charge balance from the changes of aqueous solution and magnetite. The
results suggest that,
455 in Fe²⁺-amended magnetite suspension at pH 7, AQDS promotes the transfer
of electron
456 equivalents from aqueous solution to magnetite, inhibits incorporation of Fe²⁺ or
electron injection
457 into magnetite structure, and also induces the production of non-magnetic Fe(II)
(OH)₂-like species
458 on magnetite surface.

459 In magnetite suspension (3000 μ M) without added Fe²⁺_(aq) at pH 8, no
measurable Fe²⁺_(aq) is
460 released from magnetite ([Fe²⁺_(aq)] = 0 μ M), no matter whether AQDS is
present (Table 1).

461 Addition of 100 μ M AQDS results in 80.8 μ M reduced AQDS ($2*[AQDS_{red}]_{eq} =$
161.6 μ M), and
462 correspondingly decreases x_{stru} in magnetite from 0.526 to 0.501. The
decrease of [Fe(II)_{stru}] in
463 magnetite after reaction with AQDS is ~ 159 μ M (for details of $\Delta [Fe(II)]_{stru}$
calculation, see SI
464 Section S5.3) that is close to the value of $2*[AQDS_{red}]_{eq}$ (161.6 μ M). Thus,
AQDS is reduced

465 mainly by structural Fe(II) of magnetite in this case. The value of x_{surf} slightly increases from

466 0.584 to 0.590 after AQDS addition (Table 1), implying the similar solid-
phase migration of

467 electron equivalents in magnetite that is mentioned above.

468 The amendment of 1000 $\mu\text{M Fe}^{2+}_{(\text{aq})}$ to the 3000 μM magnetite suspension
at pH 8 induces

469 the uptake of 555 $\mu\text{M Fe}^{2+}_{(\text{aq})}$ by magnetite, coupled to an increase of x_{stru}
from 0.526 to 0.538.

470 The increase of x_{stru} is attributed to the incorporation of Fe^{2+} into magnetite
structure or electron

471 transfer from sorbed Fe(II) to structural Fe(III) in the underlying magnetite.
After addition of 100

472 μM AQDS to Fe^{2+} -amended magnetite at pH 8, AQDS is completely reduced,
and $\Delta[\text{Fe}^{2+}_{(\text{aq})}]$

473 changes from -555 to -750 μM (Table 1). Correspondingly, the value of x_{stru}
(0.525) for magnetite

474 in this case is similar to that (0.526) of magnetite in the pH 8 buffer solution
without added $\text{Fe}^{2+}_{(\text{aq})}$

475 or AQDS. The increase in the absolute values of $\Delta[\text{Fe}^{2+}_{(\text{aq})}]$ (195 μM) is close
to the value of

476 $2*[\text{AQDS}_{\text{red}}]_{\text{eq}}$ (200 μM), so electron equivalents mainly flows from $\text{Fe}^{2+}_{(\text{aq})}$ to
AQDS, probably

477 via the steps involving Fe^{2+} adsorption onto magnetite surface and subsequent
AQDS reduction by

478 Fe(II)-Mt. No further $\text{Fe}^{2+}_{(\text{aq})}$ incorporation or electron injection into magnetite
structure occurred

479 after AQDS addition under this condition, even though there are excess $\text{Fe}^{2+}_{(\text{aq})}$
ions in the system.

480 Compared to the Fe^{2+} -amended magnetite without AQDS, addition of AQDS
results in the

481 decrease of both x_{stru} and x_{surf} , which is similar to the trend observed at pH 7
(Table 1). The XAS

482 signal (Figure S13) shows the similar intensity of Fe(II) peak before and after
reaction with AQDS

483 in the Fe^{2+} -amended magnetite at pH 8, suggesting the presence of non-
magnetic Fe(II) species on

484 magnetite surface. The Fe(II) enrichment into surface structure and the
formation of non-magnetic

485 Fe(II)(OH)₂-like species after AQDS addition might inhibit $\text{Fe}^{2+}_{(\text{aq})}$ incorporation or
electron

486 injection into magnetite structure at pH 8.

487

488 Environmental Implications

489 The findings in this study reveal that the model quinone molecule AQDS
can significantly

490 impact the interaction between magnetite and dissolved Fe^{2+} , causing changes
in: (i) redox

491 potentials for the Fe^{2+} -magnetite system; (ii) the equilibrium distribution of
 Fe(II) in the

492 magnetite-solution system; and (iii) the change of the structural Fe(II)/Fe(III)
versus

493 surface-localized Fe(II)/Fe(III) in magnetite, under environmentally relevant
conditions. The

494 findings show that the dynamic redistribution of electron equivalents between
 $\text{Fe}^{2+}_{(\text{aq})}$ and

495 mixed-valent iron oxide minerals, such as magnetite, can be significantly
impacted by the

496 presence of quinones, resulting in modified reduction reactivity of minerals.
The inhibition of

497 $\text{Fe}^{2+}_{(\text{aq})}$ incorporation or electron injection into magnetite structure by AQDS in
the Fe^{2+} -amended

498 magnetite suspension at pH 7-8 is consistent with our previous results that
humic acid-coated

499 magnetite transfers electrons between microbial cells of different species
mainly via humic acid

500 on magnetite surface.⁴⁹ Moreover, understanding the effect of quinones on
the flow of electron

501 equivalents in $\text{Fe}^{2+}_{(\text{aq})}$ -magnetite systems can aid understanding of the role of
magnetite in

502 biogeochemical processes and help develop applications of magnetite/zero
valent iron

503 nanoparticles for environmental remediation.

504 At the same time, the equilibrium speciation of AQDS can also be
changed, to different

505 extents, by magnetite in the absence or presence of $\text{Fe}^{2+}_{(\text{aq})}$. AQDS is usually
used as an electron

506 shuttle to promote dissimilatory microbial reduction of Fe(III) oxides.
Because magnetite and

507 $\text{Fe}^{2+}_{(\text{aq})}$ are common products of microbial Fe(III) reduction, the presence of
quinones may not

508 only facilitate electron transfer between microorganisms and iron oxides, but
also influence

509 reduction reactivity of biogenic magnetite. In addition, redox-active quinones

can act as recyclable

510 electron acceptors for anaerobic microbial respiration and become re-oxidized
during aeration of

511 temporarily anoxic systems.⁵⁰ Moreover, natural organic matters contain diverse
quinone moieties,

512 so the effect of other model quinones on Fe²⁺-magnetite interaction deserve
further exploration for

513 understanding the cycling and impacts of natural organic matters in
environmentally relevant

514 redox transition zones.

515

516 **ASSOCIATED CONTENT**

517 Supporting Information. Additional figures and details for Materials and Methods
and Results and

518 Discussion are presented. This material is available free of charge via the
Internet at

519 <http://pubs.acs.org>.

520

521 **AUTHOR INFORMATION**

522 Corresponding Author

523 J Liu: E-mail: juan.liu@pku.edu.cn; address: College of Environmental Sciences
and Engineering,

524 Peking University, Beijing 100871, China

525 Z Zhu: E-mail: zlzhu@cug.edu.cn; address: State Key Laboratory of Biogeology
and

526 Environmental Geology, School of Earth Sciences, China University of
Geosciences, Wuhan,

527 Hubei 430074, China.

528

529 **ACKNOWLEDGEMENTS**

530 This work was financially supported by National Basic Research Program
of China (973

531 Program, 2014CB846001) and National Natural Science Foundation of China
(41472306 and

532 41673014). KMR acknowledges support from the U.S. Department of Energy
(DOE), Office of
533 Science, Office of Basic Energy Sciences, from the Chemical Sciences,
Geosciences, and
534 Biosciences Division through its Geosciences program at Pacific Northwest
National Laboratory
535 (PNNL). A portion of this research was performed using EMSL, a national
scientific user facility
536 sponsored by the DOE Office of Biological and Environmental Research and
located at PNNL.
537 The work performed at the ALS is supported by the Director, Office of Basic
Energy Sciences of
538 the U.S. DOE under Contract No. DE-AC02-05CH11231.
539

540 Table 1. Charge balance in the 3000 μM magnetite suspensions amended with 0
 - 1000 μM $\text{Fe}^{2+}_{(\text{aq})}$

541 and 0 - 100 μM AQDS at pH 7-8

Experimental conditions		$\text{Fe}^{2+}_{(\text{aq})}$	AQDS	Electron equivalents [‡]	Changes in magnetite		
$\text{Fe(II)}_{\text{added}}$ (μM)	pH	[AQDS] i nt (μM)	$\Delta[\text{Fe}^{2+}_{(\text{aq})}]^{\dagger}$ (μM)	$2*[\text{AQDS}]_{\text{red}}$ d (μM)	$\Delta[\text{Fe}^{2+}_{(\text{aq})}] + 2*[\text{AQDS}]_{\text{red}}$ ed (μM)	X_{stru}^{\perp}	X_{surf}^{\top}
0	Stoc k	0	0	0	0	0.544	0.53 8
0	7	0	250.5	0	250. 5	0.498	0.60 4
0	7	100	206.7	13.4	220. 1	0.486	0.66 7
100 0	7	0	19.2	0	19.2	0.511	0.71 4
100 0	7	100	-380.0	196.0	-184	0.492	0.64 3
0	8	0	0	0	0	0.526	0.58 4
0	8	100	0	161.6	161. 6	0.501	0.59 0
100 0	8	0	-555	0	-555	0.538	0.61 8
100 0	8	100	-750	200.0	-550	0.525	0.57 4

542 [†]The positive values of $\Delta[\text{Fe}^{2+}_{(\text{aq})}]$ represent the increase of $\text{Fe}^{2+}_{(\text{aq})}$, and the
 543 negative values denote

543 the decrease of $\text{Fe}^{2+}_{(\text{aq})}$

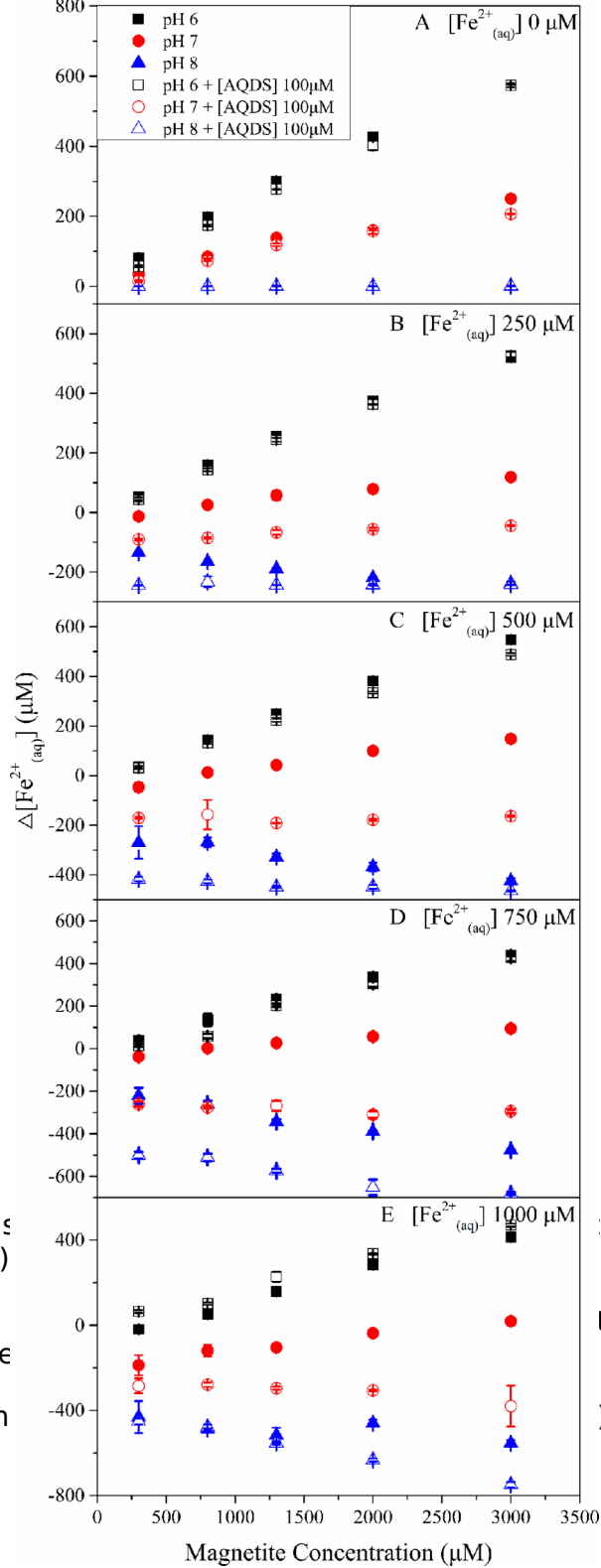
544 [‡]The positive values represent the flow of electron equivalents from aqueous
 545 solution to solid, and

545 the negative values denote the opposite direction.

546 [⊥] X_{stru} : structural Fe(II)/Fe(III) ratio deduced from μXRD results

547 [⊤] X_{surf} : surface-localized Fe(II)/Fe(III) ratio deduced from XMCD results

548



549

550 Figure 1. Comparison with 0 (A), 250 (B)

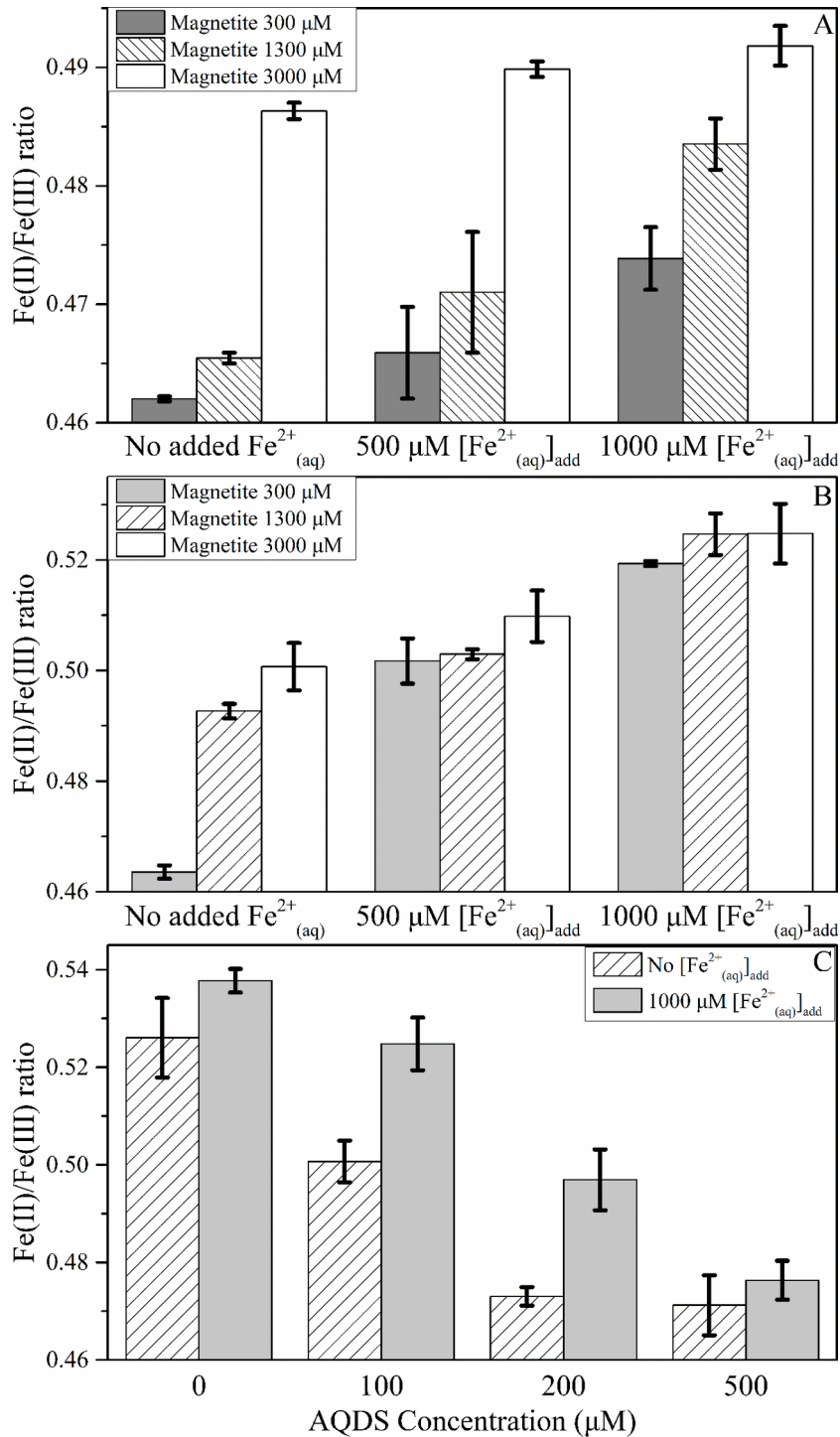
551 500 (C), 750 (D), 7 (red), and 8 (blue

552 without (solid sym

icles equilibrated

t pH 6 (black),

).



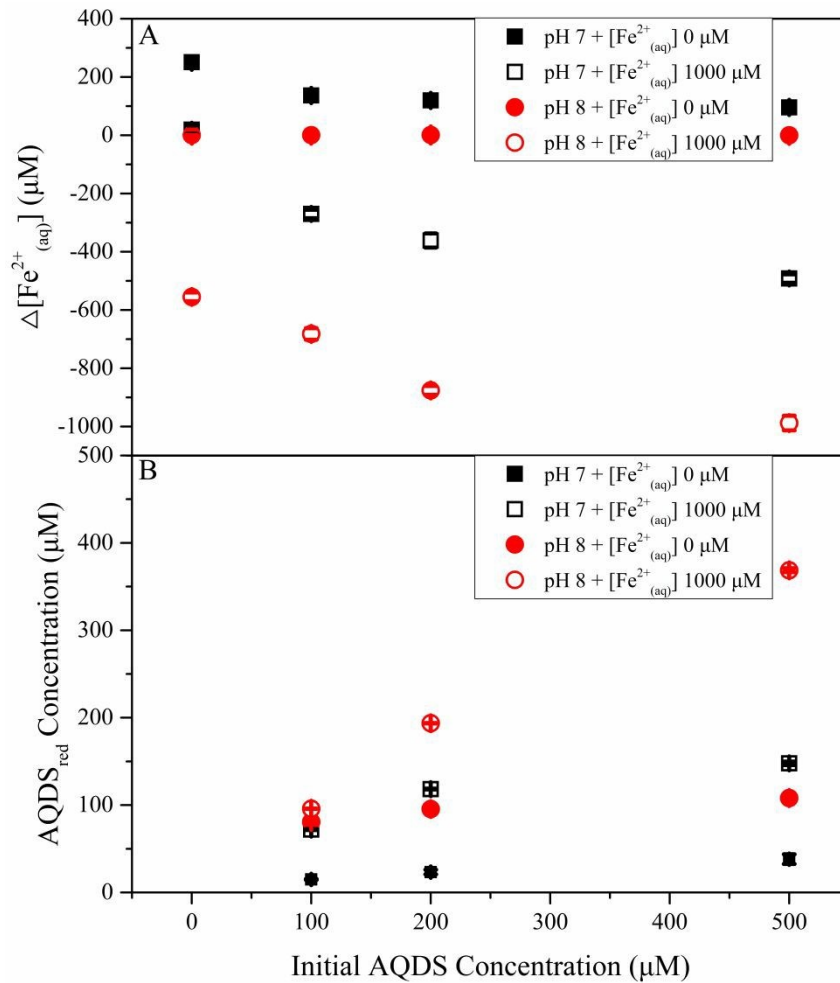
553

554 Figure 2. Structural Fe(II)/Fe(III) ratios of magnetite (300 - 3000 μM) in the suspensions amended

555 with 0-1000 μM $Fe^{2+}_{(aq)}$ at pH 7 (A) and 8 (B) with 100 μM AQDS. (C) Effects of initial AQDS

556 concentration (0-500 μM) on structural Fe(II)/Fe(III) ratios of magnetite (3000 μM) in the

557 suspensions without $Fe^{2+}_{(aq)}$ and with 1000 μM $Fe^{2+}_{(aq)}$, respectively, at pH 8.



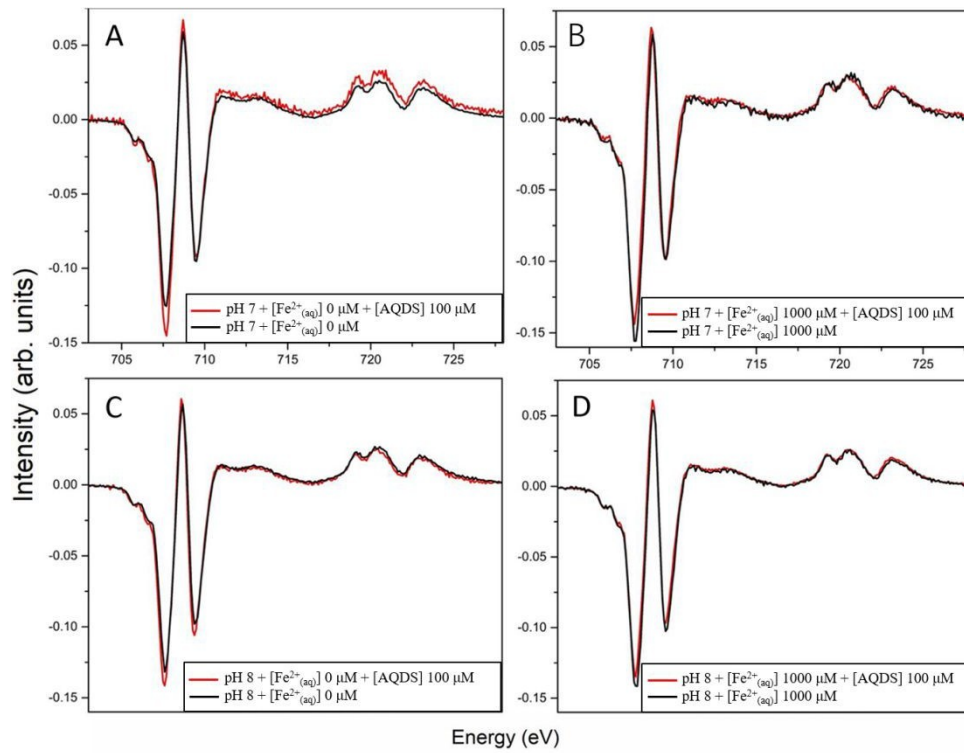
558

559 Figure 3 Effects of initial AQDS concentrations on (A) the change of $[\text{Fe}^{2+}_{(\text{aq})}]$ and (B) the

560 equilibrium concentrations of reduced AQDS in the 3000 μM magnetite suspensions without

561 added $\text{Fe}^{2+}_{(\text{aq})}$ (solid dots) or amended with 1000 μM $\text{Fe}^{2+}_{(\text{aq})}$ (open dots).

562



565

566 Figure 4 Comparison of XMCD spectra of 3000 μM magnetite NPs before (black) and after (red)

567 reaction with 100 μM AQDS in the pH 7 buffer solution without (A) or with (B) 1000 μM added

568 Fe²⁺_(aq), and in the pH 8 buffer solution without (C) or with (D) 1000 μM added Fe²⁺_(aq).

569 References

- 570 (1) Baer, D. R.; Grosz, A. E.; Ilton, E. S.; Krupka, K. M.; Liu, J.; Penn, R. L.; Pepin, A.,
571 Separation,
572 characterization and initial reaction studies of magnetite particles from Hanford
573 sediments. *Phys. Chem. Earth* **2010**, 35, (6), 233-241.
- 574 (2) Liu, J.; Pearce, C. I.; Qafoku, O.; Arenholz, E.; Heald, S. M.; Rosso, K. M.,
575 Tc(VII) reduction
576 kinetics by titanomagnetite ($\text{Fe}_{3-x}\text{Ti}_x\text{O}_4$) nanoparticles. *Geochim. Cosmochim. Acta*
577 **2012**, 92, 67-81.
- 578 (3) Latta, D. E.; Pearce, C. I.; Rosso, K. M.; Kemner, K. M.; Boyanov, M. I.,
579 Reaction of U^{VI} with
580 Titanium-Substituted Magnetite: Influence of Ti on U^{IV} Speciation. *Environ. Sci.*
581 *Technol.* **2013**, 47,
582 (9), 4121-4130.
- 583 (4) Cheng, W.; Marsac, R.; Hanna, K., Influence of Magnetite Stoichiometry on the
584 Binding of
585 Emerging Organic Contaminants. *Environ. Sci. Technol.* **2018**, 52, (2), 467-473.
- 586 (5) Ali, I., New Generation Adsorbents for Water Treatment. *Chem. Rev.* **2012**, 112,
587 (10), 5073-5091.
- 588 (6) Usman, M.; Byrne, J. M.; Chaudhary, A.; Orsetti, S.; Hanna, K.; Ruby, C.;
589 Kappler, A.;
590 Haderlein, S. B., Magnetite and Green Rust: Synthesis, Properties, and
591 Environmental Applications of
592 Mixed-Valent Iron Minerals. *Chem. Rev.* **2018**, 118, (7), 3251-3304.
- 593 (7) Zang, H.; Miao, C.; Shang, J.; Liu, Y.; Liu, J., Structural effects on the
594 catalytic activity of
595 carbon-supported magnetite nanocomposites in heterogeneous Fenton-like
596 reactions. *RSC Adv.* **2018**, 8,
597 (29), 16193-16201.
- 598 (8) Catalano, J. G.; Fenter, P.; Park, C.; Zhang, Z.; Rosso, K. M., Structure and
599 oxidation state of
600 hematite surfaces reacted with aqueous Fe(II) at acidic and neutral pH. *Geochim.*
601 *Cosmochim. Acta*
602 **2010**, 74, (5), 1498-1512.
- 603 (9) Frierdich, A. J.; Helgeson, M.; Liu, C.; Wang, C.; Rosso, K. M.; Scherer, M. M.,
604 Iron Atom
605 Exchange between Hematite and Aqueous Fe(II). *Environ. Sci. Technol.* **2015**, 49,
606 (14), 8479-8486.
- 607 (10) Cornell, R. M.; Schwertmann, U., *The Iron Oxides: Structure, Properties,*
608 *Reactions, Occurrences*
609 *and Uses*. Wiley-VCH: Weinheim, 2003.
- 610 (11) Pearce, C. I.; Qafoku, O.; Liu, J.; Arenholz, E.; Heald, S. M.; Kukkadapu, R. K.;
611 Gorski, C. A.;
612 Henderson, C. M. B.; Rosso, K. M., Synthesis and properties of titanomagnetite ($\text{Fe}_{3-x}\text{Ti}_x\text{O}_4$)
613 nanoparticles: A tunable solid-state Fe(II/III) redox system. *J. Colloid Interface Sci.*

- 2012, 387, (1),
597 24-38.
- 598 (12) Klausen, J.; Troeber, S. P.; Haderlein, S. B.; Schwarzenbach, R. P., Reduction of Substituted
599 Nitrobenzenes by Fe(II) in Aqueous Mineral Suspensions. *Environ. Sci. Technol.*
1995, 29, (9),
600 2396-2404.
- 601 (13) Gregory, K. B.; Larese-Casanova, P.; Parkin, G. F.; Scherer, M. M., Abiotic Transformation of
602 Hexahydro-1,3,5-trinitro-1,3,5-triazine by Fe^{II} Bound to Magnetite. *Environ. Sci. Technol.* **2004**, 38, 603 (5), 1408-1414.
- 604 (14) Gorski, C. A.; Scherer, M. M., Influence of Magnetite Stoichiometry on Fe^{II} Uptake and
605 Nitrobenzene Reduction. *Environ. Sci. Technol.* **2009**, 43, (10), 3675-3680.
- 606 (15) Gorski, C. A.; Handler, R. M.; Beard, B. L.; Pasakarnis, T.; Johnson, C. M.; Scherer, M. M., Fe
607 Atom Exchange between Aqueous Fe²⁺ and Magnetite. *Environ. Sci. Technol.* **2012**, 46, (22), 608 12399-12407.
- 609 (16) Liu, J.; Pearce, C. I.; Liu, C.; Wang, Z.; Shi, L.; Arenholz, E.; Rosso, K. M., Fe_{3-x}Ti_xO₄
610 Nanoparticles as Tunable Probes of Microbial Metal Oxidation. *J. Am. Chem. Soc.* **2013**, 135, (24),

- 611 8896-8907.
- 612 (17) Byrne, J. M.; Klueglein, N.; Pearce, C.; Rosso, K. M.; Appel, E.; Kappler, A., Redox cycling of Fe(II) and Fe(III) in magnetite by Fe-metabolizing bacteria. *Science* **2015**, 347, (6229), 1473-1476. 614 (18) Peng, H.; Pearce, C.; Huang, W.; Zhu, Z.; N'Diaye, A. T.; Rosso, K.; Liu, J., Reversible Fe(II) Uptake/Release by Magnetite Nanoparticles. *Environ. Sci.: Nano* **2018**, 5, (7), 1545-1555.
- 616 (19) Frierdich, A. J.; Beard, B. L.; Scherer, M. M.; Johnson, C. M., Determination of the Fe(II)_{aq}-magnetite equilibrium iron isotope fractionation factor using the three-isotope method and a multi-direction approach to equilibrium. *Earth. Planet. Sci. Lett.* **2014**, 391, 77-86.
- 619 (20) Handler, R. M.; Frierdich, A. J.; Johnson, C. M.; Rosso, K. M.; Beard, B. L.; Wang, C.; Latta, D. E.; Neumann, A.; Pasakarnis, T.; Premaratne, W. A. P. J.; Scherer, M. M., Fe(II)-Catalyzed Recrystallization of Goethite Revisited. *Environ. Sci. Technol.* **2014**, 48, (19), 11302-11311.
- 622 (21) Gorski, C. A.; Fantle, M. S., Stable mineral recrystallization in low temperature aqueous systems: A critical review. *Geochim. Cosmochim. Acta* **2017**, 198, 439-465.
- 624 (22) Shi, Z.; Zachara, J. M.; Shi, L.; Wang, Z.; Moore, D. A.; Kennedy, D. W.; Fredrickson, J. K., Redox Reactions of Reduced Flavin Mononucleotide (FMN), Riboflavin (RBF), and Anthraquinone-2,6-disulfonate (AQDS) with Ferrihydrite and Lepidocrocite. *Environ. Sci. Technol.* **2012**, 46, (21), 11644-11652.
- 628 (23) Orsetti, S.; Laskov, C.; Haderlein, S. B., Electron Transfer between Iron Minerals and Quinones: Estimating the Reduction Potential of the Fe(II)-Goethite Surface from AQDS Speciation. *Environ. Sci. Technol.* **2013**, 47, (24), 14161-14168.
- 631 (24) Fan, D.; Bradley, M. J.; Hinkle, A. W.; Johnson, R. L.; Tratnyek, P. G., Chemical Reactivity Probes for Assessing Abiotic Natural Attenuation by Reducing Iron Minerals. *Environ. Sci. Technol.* **2016**, 50, (4), 1868-1876.
- 634 (25) Lovley, D. R.; Coates, J. D.; Blunt-Harris, E. L.; Phillips, E. J. P.; Woodward, J. C., Humic substances as electron acceptors for microbial respiration. *Nature* **1996**, 382, (6590), 445-448.
- 636 (26) Newman, D. K.; Kolter, R., A role for excreted quinones in extracellular electron transfer. *Nature* **2000**, 405, (6782), 94-97.
- 638 (27) Shimizu, M.; Zhou, J.; Schröder, C.; Obst, M.; Kappler, A.; Borch, T., Dissimilatory Reduction and Transformation of Ferrihydrite-Humic Acid Coprecipitates. *Environ. Sci. Technol.* **2013**, 47, (23), 13375-13384.
- 641 (28) Shi, Z.; Zachara, J. M.; Wang, Z.; Shi, L.; Fredrickson, J. K., Reductive dissolution of goethite and hematite by reduced flavins. *Geochim. Cosmochim. Acta* **2013**, 121, 139-154.
- 643 (29) Gorski, C. A.; Nurmi, J. T.; Tratnyek, P. G.; Hofstetter, T. B.; Scherer, M. M., Redox Behavior of Magnetite: Implications for Contaminant Reduction. *Environ. Sci. Technol.* **2010**, 44, (1), 55-60.
- 645 (30) Dhakal, P.; Matocha, C. J.; Huggins, F. E.; Vandivere, M. M., Nitrite Reactivity with Magnetite. *Environ. Sci. Technol.* **2013**, 47, (12), 6206-6213.
- 647 (31) Bae, S.; Lee, W., Influence of Riboflavin on Nanoscale Zero-Valent Iron Reactivity during the Degradation of Carbon Tetrachloride. *Environ. Sci. Technol.* **2014**, 48, (4), 2368-2376.
- 649 (32) Bae, S.; Hanna, K., Reactivity of Nanoscale Zero-Valent Iron in Unbuffered Systems: Effect of

- 650 pH and Fe(II) Dissolution. *Environ. Sci. Technol.* **2015**, 49, (17), 10536-10543.
- 651 (33) Shi, Z.; Fan, D.; Johnson, R. L.; Tratnyek, P. G.; Nurmi, J. T.; Wu, Y.; Williams, K. H., Methods 652 for characterizing the fate and effects of nano zerovalent iron during groundwater remediation. *J. 653 Contam. Hydrol.* **2015**, 181, 17-35.
- 654 (34) Marsac, R.; Pasturel, M.; Hanna, K., Reduction Kinetics of Nitroaromatic Compounds by

- 655 Titanium-Substituted Magnetite. *J. Phys. Chem. C* **2017**, 121, (21), 11399-11406.
- 656 (35) Stookey, L. L., Ferrozine — a new spectrophotometric reagent for iron. *Anal. Chem.* **1970**, 42, (7), 779-781.
- 657 (36) Yu, Q.; Kandedgedara, A.; Xu, Y.; Rorabacher, D. B., Avoiding Interferences from Good's Buffers: A Contiguous Series of Noncomplexing Tertiary Amine Buffers Covering the Entire Range of 660 pH 3–11. *Anal. Biochem.* **1997**, 253, (1), 50-56.
- 661 (37) Buchholz, A.; Laskov, C.; Haderlein, S. B., Effects of Zwitterionic Buffers on Sorption of Ferrous
- 662 Iron at Goethite and Its Oxidation by CCl₄. *Environ. Sci. Technol.* **2011**, 45, (8), 3355-3360.
- 663 (38) Liu, C.; Zachara, J. M.; Foster, N. S.; Strickland, J., Kinetics of Reductive Dissolution of
- 664 Hematite by Bioreduced Anthraquinone-2,6-disulfonate. *Environ. Sci. Technol.* **2007**, 41, (22), 7730-7735.
- 665 (39) Uchimiya, M.; Stone, A. T., Reduction of Substituted *p*-Benzoquinones by Fe^{II} Near Neutral pH. *Aquat. Geochem.* **2009**, 16, (1), 173-188.
- 666 (40) Stewart, S. M.; Hofstetter, T. B.; Joshi, P.; Gorski, C. A., Linking Thermodynamics to Pollutant
- 667 Reduction Kinetics by Fe²⁺ Bound to Iron Oxides. *Environ. Sci. Technol.* **2018**, 52, (10), 5600-5609.
- 668 (41) Pang, S. C.; Chin, S. F.; Anderson, M. A., Redox equilibria of iron oxides in aqueous-based magnetite dispersions: Effect of pH and redox potential. *J. Colloid Interface Sci.* **2007**, 311, (1), 94-101.
- 669 (42) Wedege, K.; Dražević, E.; Konya, D.; Bentien, A., Organic Redox Species in Aqueous Flow
- 670 Batteries: Redox Potentials, Chemical Stability and Solubility. *Sci. Rep.* **2016**, 6, 39101.
- 671 (43) Clark, W. M., *Oxidation-Reduction Potentials of Organic Systems*. Williams and Wilkins: Baltimore, MD, 1960.
- 672 (44) Rosso, K. M.; Smith, D. M. A.; Wang, Z.; Ainsworth, C. C.; Fredrickson, J. K., Self-Exchange Electron Transfer Kinetics and Reduction Potentials for Anthraquinone Disulfonate. *J. Phys. Chem. A* **2004**, 108, (16), 3292-3303.
- 673 (45) Gorski, Christopher, A.; Scherer, Michelle, M., Determination of nanoparticulate magnetite stoichiometry by Mössbauer spectroscopy, acidic dissolution, and powder X-ray diffraction: A critical review. *Am. Mineral.* **2010**, 95, (7), 1017-1026.
- 674 (46) Sander, M.; Hofstetter, T. B.; Gorski, C. A., Electrochemical Analyses of Redox-Active Iron Minerals: A Review of Nonmediated and Mediated Approaches. *Environ. Sci. Technol.* **2015**, 49, (10), 5862-5878.
- 675 (47) Uchimiya, M.; Stone, A. T., Redox reactions between iron and quinones: Thermodynamic
- 676 constraints. *Geochim. Cosmochim. Acta* **2006**, 70, (6), 1388-1401.
- 677 (48) Jones, A. M.; Murphy, C. A.; Waite, T. D.; Collins, R. N., Fe(II) Interactions with Smectites: Temporal Changes in Redox Reactivity and the Formation of Green Rust. *Environ. Sci. Technol.* **2017**, 51, (21), 12573-12582.
- 678 (49) You, Y.; Zheng, S.; Zang, H.; Liu, F.; Liu, F.; Liu, J., Stimulatory effect of magnetite on the syntrophic metabolism of *Geobacter* co-cultures: Influences of surface coating. *Geochim. Cosmochim. Acta* **2018**.
- 679 (50) Klupfel, L.; Piepenbrock, A.; Kappler, A.; Sander, M., Humic substances as fully regenerable
- 680 electron acceptors in recurrently anoxic environments. *Nat. Geosci.* **2014**, 7, (3), 195-200.
- 681
- 682
- 683
- 684
- 685
- 686
- 687
- 688
- 689
- 690
- 691
- 692
- 693
- 694
- 695
- 696